

Excited States of the Phthalimide Chromophore and Their Exciton Couplings: A Tool for Stereochemical Assignments

Jacek Gawronski,^{*,†} Franciszek Kazmierczak,[†] Krystyna Gawronska,[†]
 Urszula Rychlewska,[†] Bengt Nordén,[‡] and Anders Holmén^{*,‡}

Contribution from the Department of Chemistry, A. Mickiewicz University, 60-780 Poznań, Poland, and
 Department of Physical Chemistry, Chalmers University of Technology, S-412 96 Göteborg, Sweden

Received June 19, 1998

Abstract: The electronically excited states of the phthalimide chromophore have been studied by means of linear dichroism (LD) of samples partially oriented in poly(vinyl alcohol) films, magnetic circular dichroism (MCD), and circular dichroism (CD) spectroscopy. On the basis of the LD measurements, the low-energy tail (340–320 nm) of the first absorption band is assigned to an out-of-plane polarized $n \rightarrow \pi^*$ transition (I). At higher energy, the electronic spectrum is resolved into contributions from five $\pi \rightarrow \pi^*$ transitions: II (300 nm, long-axis polarized), III (275 nm, short-axis polarized), IV (235 nm, short-axis polarized), V (220 nm, long-axis polarized), and VI (\sim 210 nm, short-axis polarized). The results from semiempirical (INDO/S-CI) and ab initio (CIS/6-31+G(d)) MO calculations compare well with the proposed assignments of the excited states. Degenerate exciton interaction between electric-dipole-allowed transitions of two phthalimide chromophores is observed in the electronic absorption spectra of the achiral bis-phthalimides **2a–c** and in the CD spectrum of the chiral bis-phthalimide **3a**. For the latter compound, the solid-state geometry has been determined by X-ray diffraction analysis. Good agreement between experimental and computed CD spectra confirms that the coupled-oscillator exciton model provides the basis for a reliable nonempirical method for the assignment of absolute configuration for this class of compounds. Nondegenerate exciton coupling between phthalimide and benzoate or phenyl chromophores is born out in the CD spectra of homochiral molecules **3c** and **3d** with the rigid cyclohexane skeleton. Finally, the exciton coupling method is used to make stereochemical assignments for the acyclic, conformationally flexible derivatives **4a–c** and **5b**.

Introduction

Phthalimide (1*H*-isoindole-1,3(2*H*)-dione) (**1a**) and its *N*-substituted derivatives constitute an important class of heteroaromatic compounds, due to the feasibility of forming the imide ring by the reaction of amines and related compounds with phthalic anhydride, phthalic dichloride, or *N*-(alkoxycarbonyl)phthalimides. In synthetic organic chemistry, masked nitrogen nucleophiles derived from **1a** are widely used in substitution and addition reactions.¹ Phthalimides constitute convenient and widely used forms of protected primary amines.² Recently, the phthalimidomethyl group has been used for protection of thiols.³ Finally, it may be noted that polyphthalimides exhibit interesting nonlinear optical properties.⁴

Despite extensive use and interest in the phthalimide derivatives, their electronic spectra have not been fully clarified.^{5–7} From studies of the photophysical and photochemical properties,^{8,9} it has been suggested that the lowest excited singlet state of *N*-alkylated phthalimides is an $n\pi^*$ state, but this has never been unambiguously proven. For the higher energy transitions, reliable experimental assignments are missing. Some early ORD^{10–12} and CD¹³ data of chiral phthalimides were reported but without clear-cut conclusions on the nature of the transitions and their relation to the structure. Since the phthalimide chromophore has effectively C_{2v} symmetry¹⁴ any transition

* To whom correspondence should be addressed. E-mail: holmen@phc.chalmers.se. Phone: +46 31 772 3049. Fax: +46 31 772 3858.

[†] Mickiewicz University.

[‡] Chalmers University of Technology.

(1) Recent examples: (a) Bunt, R. C.; Trost, B. M. *J. Am. Chem. Soc.* **1994**, *116*, 4089. (b) Ramesh, N. G.; Balasubramanian, K. K. *Tetrahedron* **1995**, *51*, 255. (c) Barrett, A. G. M.; Rys, D. J. *J. Chem. Soc., Perkin Trans. I* **1995**, 1009.

(2) (a) Wolman, Y. In *The Chemistry of the Amino Group*; Patai, S., Ed.; Wiley: New York, 1968; Chapter 11. (b) Barton, J. W. In *Protective Groups in Organic Chemistry*; McOmie, J. F. W., Ed.; Plenum: London, 1973, Chapter 2. (c) Greene, T. W.; Wuts, P. G. M. *Protective Groups in Organic Synthesis*, 2nd ed.; Wiley: New York, 1991; Chapter 7. (d) Kunz, H.; Waldmann, H. In *Comprehensive Organic Synthesis*; Trost, B. M., Fleming, I., Eds.; Pergamon: Oxford, 1991; Chapter 6.3.1. (e) Kocienski, P. J. *Protecting Groups*; Thieme: Stuttgart, 1994; Chapter 6.2.1.

(3) Gong, Y.-D.; Iwasawa, N. *Chem. Lett.* **1994**, 2139.

(4) (a) Yu, D.; Gharavi, A.; Yu, L. *J. Am. Chem. Soc.* **1995**, *117*, 11680. (b) Chen, T.-A.; Jen, A. K.-Y.; Cai, Y. *Ibid.* **1995**, *117*, 7295.

(5) Galasso, V.; Pappalardo, G. C. *J. Chem. Soc., Perkin Trans. 2*, **1976**, 574.

(6) (a) Perkampus, H.-H. *UV-Vis Atlas of Organic Compounds*; Verlag Chemie: Weinheim, 1992; p 914. (b) Ames, D. E.; Grey, T. F. *J. Chem. Soc.* **1955**, 3518.

(7) (a) Fabian, W. *J. Mol. Struct. (THEOCHEM)* **1982**, *90*, 249. (b) Fabian, W. *Z. Naturforsch.* **1980**, *35a*, 865.

(8) (a) Nurmuchametov, R. N.; Bielays, I. L.; Shigorin, D. N. *Zh. Fiz. Khim.* **1967**, *41*, 1928. (b) Nurmuchametov, R. N.; Semenova, L. I.; Korolkova, N. V.; Valkova, G. A.; Ponomaryev, I. I. *Zh. Fiz. Khim.* **1990**, *64*, 2972.

(9) (a) Coyle, J. D.; Newport, G. L.; Harriman, A. *J. Chem. Soc., Perkin Trans. 2* **1978**, 133. (b) Coyle, J. D.; Harriman, A.; Newport, G. L.; *J. Chem. Soc., Perkin Trans. 2* **1979**, 799.

(10) Brewster, J. H.; Osman, S. F. *J. Am. Chem. Soc.* **1960**, *82*, 5754.

(11) La Manna, A.; Ghislandi, V. *Il Farmaco* **1964**, *19*, 480.

(12) (a) Djerassi, C.; Lund, E.; Bunnenberg, E.; Sheehan, J. C. *J. Org. Chem.* **1961**, *26*, 4509. (b) Wolf, H.; Bunnenberg, E.; Djerassi, C. *Chem. Ber.* **1964**, *97*, 533.

(13) Berova, N.; Tinchev, L. *Izv. Khim.* **1976**, *9*, 551 (*Chem. Abstr.* **1977**, *87*, 183838t).

(14) Structure by X-ray diffraction: (a) Matzat, E. *Acta Crystallogr.* **1972**, *B28*, 415. (b) Weng Ng, S. *Ibid.* **1992**, *C48*, 1694.

($\pi \rightarrow \pi^*$ or $n \rightarrow \pi^*$ in the UV region) should be polarized along the symmetry axes or perpendicular to a reflection plane. From semiempirical INDO/S-CI calculations,⁵ it has been concluded that the strong band ($\epsilon \approx 36000 \text{ M}^{-1} \text{ cm}^{-1}$) observed experimentally at about 220 nm in *N*-substituted phthalimides corresponds to the $\pi \rightarrow \pi^*$ charge-transfer transition analogous to the charge-transfer transitions in benzoates and benzamides.

Due to its symmetry, phthalimide can be seen as an obvious and nearly perfect chromophoric derivative of the amino group. Recently, we have used the 220 nm transition in circular dichroism (CD) studies to assess absolute configurations of chiral *N*-phthaloyl derivatives. As a result of nondegenerate exciton coupling between the strong electric-dipole transitions of the chirally arranged phthalimide and benzoate or phenyl chromophores, strong bisignate Cotton effects were observed, whose sign was found to correctly reflect the absolute configuration¹⁵ and even conformation¹⁶ of the molecules. This approach has also been applied to the CD spectra of di- and tetrachlorophthalimides.¹⁷

To resolve the ambiguities regarding the number of transitions and their electronic origin and polarizations, we studied the linear dichroism (LD) of *N*-alkylated phthalimides **1b** and **1c** oriented in stretched poly(vinyl alcohol) or polyethylene films. The orientation axes and order parameters of the phthalimides in the stretched films have been determined by polarized FTIR spectroscopy. Magnetic circular dichroism (MCD) and CD measurements have also been used to provide information of relative polarization angles. The experimental results are compared with the results from INDO/S-CI and ab initio CIS/6-31+G(d) calculations.

Finally, to demonstrate the application of the determined transition moments for nonempirical analysis of absolute configuration, we analyze the degenerate coupled-oscillator CD spectra of bis-phthalimides **3a** and **4a**, and we show the effect of molecular geometry on the UV spectra of achiral bis-phthalimides **2a–d**. The nondegenerate exciton coupling of model chiral cyclic (**3c**, **3d**) and acyclic (**4b**, **4c**) phthalimides bearing phenyl or benzoate groups as a second chromophore is also discussed. An application of the CD spectroscopy to determine the absolute configuration of the acyclic phthalimido-benzoate **5b** is reported.

Materials and Experimental Methods

Chemicals. The preparation and characterization of compounds **1a–d**, **2a–d**, **3a–d**, **4a–c**, and **5b** is described in Supporting Information. All aqueous solutions were prepared from deionized water (Millipore). All organic solvents were of spectrophotometric grade. Poly(vinyl alcohol) (PVA) was obtained as powder from E. I. du Pont de Nemours Co. (Elvanol).

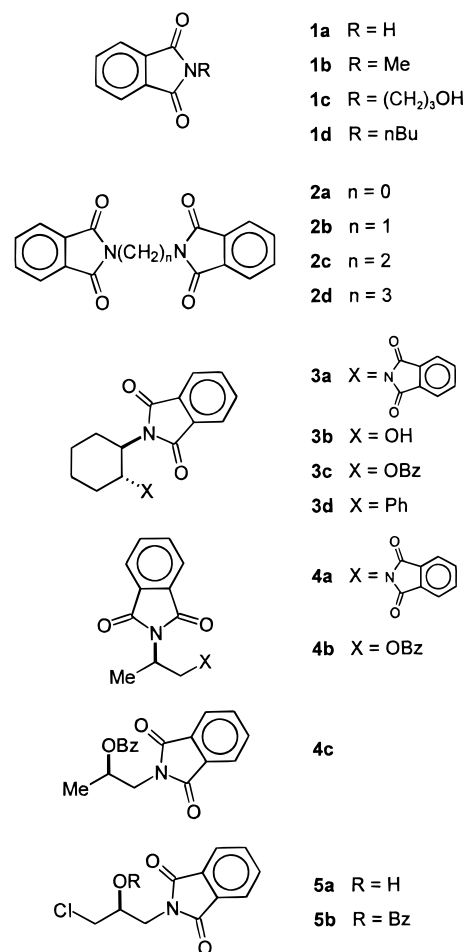
X-ray Crystallography. Crystal data and details of crystal structure determination for **3a** ($\text{C}_{22}\text{H}_{18}\text{N}_2\text{O}_4$, M_r 374.4): crystal system monoclinic; space group C2; unit cell parameters, $a = 14.362(3)$, $b = 8.599(2)$, $c = 15.239(3)$ Å, $\beta = 100.96(3)^\circ$, $V = 1847.7(9)$ Å³, Z (number of molecules in the unit cell) = 4, $D_c = 1.346 \text{ g cm}^{-3}$, μ for Cu K α radiation = 0.77 mm^{-1} . The diffraction intensities have been measured on a four-circle KM-4 (KUMA-Diffraction) diffractometer using graphite monochromated CuK α radiation in a 2θ range 1 to 130° . The structure was determined by direct methods¹⁸ and refined on F^2 by a least-squares procedure¹⁹ to the final R value of 0.041 for 2250 observed ($F_o > 4\sigma(F_o)$) reflections ($wR(F^2) = 0.124$ for all reflections). Hydrogen

(15) Kazmierczak, F.; Gawronski, K.; Rychlewska, U.; Gawronski, J. *Tetrahedron: Asymmetry* **1994**, *5*, 527.

(16) Gawronski, J.; Rozwadowska, M. D.; Kazmierczak, F. *Pol. J. Chem.* **1994**, *68*, 2279.

(17) Gawronski, J.; Kazmierczak, F.; Gawronski, K.; Skowronek, P.; Waluk, J.; Marczyk, J. *Tetrahedron* **1996**, *52*, 13201.

Chart 1



atoms have been placed in calculated positions and refined using a riding model with an isotropic temperature factor 1.2 times U_{eq} of the atom to which they are bonded. Siemens Stereochemical Workstation was used to prepare drawings.²⁰ The final atomic coordinates with equivalent isotropic temperature factors have been deposited at the Cambridge Structural Data Base together with the tables of anisotropic displacement parameters, bond lengths and angles, and H-atom coordinates.

IR and UV Linear Dichroism (LD). Polarized IR measurements were performed on a Perkin-Elmer 1800 FTIR spectrophotometer. To obtain polarized IR radiation, a KRS-5 polarizer (IGP225 Cambridge Physical Sciences) was placed in front of the sample. The spectral resolution was 2 cm^{-1} and each spectrum an average of 300 scans. Polarized UV measurements were performed on a CARY 4 spectrophotometer equipped with Glan-prism polarizers. Five data points per nanometer were collected. The preparation of stretched PVA and PE films for IR and UV measurements have been reported previously.^{21,22}

The reduced linear dichroism, LD^r , was calculated according to²³

$$LD^r(\lambda) = (A_{\parallel}(\lambda) - A_{\perp}(\lambda)) / (A_{\parallel}(\lambda) + 2A_{\perp}(\lambda)) \quad (1)$$

where $A_{\parallel}(\lambda)$ and $A_{\perp}(\lambda)$ are the absorbances measured with plane polarized light, respectively, parallel and perpendicular to the macro-

(18) Sheldrick, G. M. SHELXS-86, University of Göttingen, 1986.

(19) Sheldrick, G. M. SHELXL-93, University of Göttingen, 1993.

(20) *Stereochemical Workstation Operation Manual*, Release 3.4, Siemens Analytical X-ray Instruments, Inc., Madison, WI, USA, 1989.

(21) Holmén, A. *J. Phys. Chem.* **1997**, *101*, 4361.

(22) Holmén, A.; Broo, A.; Nordén, B.; Albinsson, B. *J. Am. Chem. Soc.* **1997**, *119*, 12240.

(23) Michl, J.; Thulstrup, E. W. *Spectroscopy with Polarized Light: Solute Alignment by Photoselection, in Liquid Crystals, Polymers, and Membranes*; VCH Publishers: New York, 1986.

scopic sample axis (the stretching direction). For a planar molecule, the LD^r for a transition *i* can be written²⁴

$$LD_i^r = 3(S_{yy} \sin^2 \theta_i + S_{zz} \cos^2 \theta_i) \quad (\text{in-plane transition}) \quad (2)$$

$$LD_i^r = 3S_{xx} \quad (\text{out-of-plane transition}) \quad (3)$$

where S_{zz} , S_{yy} , and S_{xx} are the Saupe orientation parameters²⁵ for the diagonal in-plane axes *z* and *y*, and the out-of-plane axis *x*, characterizing the orientation of the solute molecules, and θ_i is the angle between the transition dipole moment and the preferred molecular orientation axis *z*. The orientation parameters are interrelated according to

$$3S_{yy} \leq LD^r (\text{in-plane}) \leq 3S_{zz} \quad (4)$$

$$S_{xx} + S_{yy} + S_{zz} = 0 \quad (5)$$

The pure reduced linear dichroism LD_{*i*}^r is determined by using a trial-and-error method (TEM) originally proposed by Thulstrup, Eggers, and Michl.²⁶ This method is based on forming linear combinations of the type $A_i(\lambda) - dA_i(\lambda)$ with varying values of the reduction coefficient, *d*. The reduction coefficient, *d_i*, for which a specific spectral feature, *i*, disappears is related to the LD_{*i*}^r of the transition containing that feature by:²⁷

$$LD_i^r = 3 \frac{d_i - 1}{d_i + 2} \quad (6)$$

The reduction coefficients were also used to calculate the reduced spectra corresponding to the long-axis (A_1 symmetry) and short-axis (B_2 symmetry) polarized absorption intensities as outlined by Michl and Thulstrup.²³

Circular Dichroism (CD). The CD is defined as the differential absorption of two circularly polarized light beams:

$$CD(\lambda) = A_l(\lambda) - A_r(\lambda) \quad (7)$$

where $A_l(\lambda)$ and $A_r(\lambda)$ are the absorption intensities with left and right circularly polarized light. The measurements were made on an AVIV spectropolarimeter.

Magnetic Circular Dichroism (MCD) measurements were made on a JASCO 720 spectropolarimeter equipped with a permanent horse shoe magnet. The magnetic field was calibrated to be 1.1 T by using the MCD signal at 510 nm of a 1 M solution of CoSO₄ ($\Delta\epsilon_{510} = -1.88 \times 10^{-2} \text{ M}^{-1} \text{ cm}^{-1} \text{ T}^{-1}$).²⁸

Quantum-Chemical Calculations. The molecular orbital (MO) calculations of electronic absorption spectra were performed with the INDO/S model Hamiltonian.²⁹ The two-center electron repulsion integrals were calculated using the Mataga–Nishimoto scheme.³⁰ The parameters proposed in ref 29 were used except for the resonance integral β for oxygen (β_O) for which we used the value of -45 eV proposed by Del Bene and Jaffé.³¹ This modification of the standard value of β_O (-34 eV)²⁹ was suggested in a recent article by Xu and Clark dealing with INDO/S calculations of the electronic spectrum of the glycouril chromophore.³²

(24) Nordén, B. *Appl. Spectrosc. Rev.* **1978**, *14*, 157.

(25) Saupe, A. *Mol. Cryst.* **1966**, *1*, 527.

(26) (a) Thulstrup, E. W.; Michl, J.; Eggers, J. H. *J. Phys. Chem.* **1970**, *74*, 3868 (b) Michl, J.; Thulstrup, E. W.; Eggers, J. H. *J. Phys. Chem.* **1970**, *74*, 3878.

(27) Albinsson, B.; Kubista, M.; Sandros, K.; Nordén, B. *J. Phys. Chem.* **1990**, *94*, 4006.

(28) McCaffery, A. J.; Stephens, P. J.; Schatz, P. N. *Inorg. Chem.* **1967**, *9*, 1614.

(29) (a) Ridley, J.; Zerner, M. C. *Theor. Chim. Acta* **1973**, *32*, 111. Ridley, J.; Zerner, M. C. *Theor. Chim. Acta* **1976**, *42*, 223. Bacon, A. D.; Zerner, M. C. *Theor. Chim. Acta* **1979**, *53*, 21. Zerner, M. C.; Loew, G. H.; Kirchner, R. F.; Mueller-Westerhoff, U. T. *J. Am. Chem. Soc.* **1980**, *102*, 589.

(30) Del Bene, J.; Jaffé, H. H. *J. Chem. Phys.* **1968**, *48*, 4050.

(31) Xu, S. Clark, L. B. *J. Am. Chem. Soc.* **1995**, *117*, 4379.

(32) Nishimoto, K.; Mataga, N. *Z. Phys. Chem.* **1957**, *12*, 335.

In the configuration interaction (CI) calculation, all singly excited (singlet) configurations using the 17 highest occupied and 7 lowest unoccupied MO's were included. The CI space thus includes all π , n , and π^* orbitals and also the σ orbitals contributing to electronic transitions with an energy less than 50000 cm⁻¹. Expansion of the CI space was tested, but the effects on calculated spectra were negligible. We also performed calculations in order to simulate the electronic spectrum of **1b** in water solution. This was performed in a self-consistent reaction field (SCRF) calculation with the molecule embedded in a spherical cavity surrounded by a solvent continuum characterized by the dielectric constant and refractive index of water ($\epsilon = 78$, $n = 1.333$). We used the SCRF model B and the mass density approach to determine the cavity radius ($a_0 = 3.99 \text{ \AA}$), both developed by Karelson and Zerner to be used in connection with the INDO/S model Hamiltonian.³³ Electronic absorption spectra were also calculated ab initio using configuration interaction with single substitutions (CIS) and the 6-31+G(d) basis set. The active space consisted of all occupied valence orbitals and all virtual orbitals. The Gaussian 94 program was used for these calculations.³⁴ The molecular geometries used in the INDO/S and CIS/6-31+G(d) calculations were calculated with DFT-(B3LYP)/6-31G(d,p) method.

The conformational preference of the bisphthalimide **4a** was investigated by molecular mechanics calculations (MM+) using the Hyperchem program on a PC.³⁵ The lowest energy structures of each of the (–)-gauche, (+)-gauche, and trans conformations were selected for full geometry optimization at the AM1 and HF/6-31+G(d) levels of theory with the Gaussian 94 program package. These calculations were performed on the Origin 2000 computer at Chalmers University of Technology.

Results and Discussion

In this section we first present the results from the polarized spectroscopy measurements on various *N*-substituted phthalimides. Second, the experimental results are compared to calculated electronic transitions. Third, the absorption spectra of dimeric nonchiral phthalimide derivatives are analyzed with respect exciton coupling. Finally, we present some applications of degenerate and nondegenerate exciton coupling in chiral phthalimides for the assignment of stereochemistry and conformational preferences in chiral rigid and flexible bis-chromophoric systems.

Linear Dichroism, Magnetic Circular Dichroism, and Circular Dichroism of Mono-Phthalimide Derivatives. The UV absorption (A_{iso}) and reduced linear dichroism (LD^r) spectra of *N*-methylphthalimide (**1b**) oriented in stretched PVA film are shown Figure 1a. Phthalimide (**1a**) and its *N*-methyl and *N*-hydroxypropyl derivatives **1b** and **1c** have very similar absorption and LD^r spectra (Figure 1a), indicating similar modes of orientation for all three molecules. Also, *N*-butylphthalimide (**1d**) dissolved in stretched PE film (Figure 2) has A_{iso} and LD^r spectra similar to those of **1a–c** in stretched PVA film. However, the vibrational structure in the spectra is more pronounced for **1d** dissolved in the nonpolar PE film than for **1a–c** in the polar PVA film. For **1c** it was possible to measure both the polarized UV spectra (LD^r shown in Figure 1a) and polarized IR spectra (Figure 3) on the same film. In the IR spectrum of **1c** there are two strong absorptions at 1770 and 1710 cm⁻¹ which have been assigned to the in-phase and out-

(33) Karelson, M. M.; Zerner, M. C. *J. Phys. Chem.* **1992**, *96*, 6949.

(34) Gaussian 94, Revision E. 2, Frisch, M. J.; Trucks, G. W.; Schlegel, H. B.; Gill, P. M. W.; Johnson, B. G.; Robb, M. A.; Cheeseman, J. R.; Keith, T.; Petersson, G. A.; Montgomery, J. A.; Raghavachari, K.; Al-Laham, M. A.; Zakrzewski, V. G.; Ortiz, J. V.; Foresman, J. B.; Cioslowski, J.; Stefanov, B. B.; Nanayakkara, A.; Challacombe, M.; Peng, C. Y.; Ayala, P. Y.; Chen, W.; Wong, M. W.; Andres, J. L.; Replogle, E. S.; Gomperts, R.; Martin, R. L.; Fox, D. J.; Binkley, J. S.; Defrees, D. J.; Baker, J.; Stewart, J. P.; Head-Gordon, M.; Gonzalez, C.; Pople, J. A. Gaussian, Inc., Pittsburgh, PA, 1995.

(35) Hyperchem release 5, Hypercube Inc., 1997.

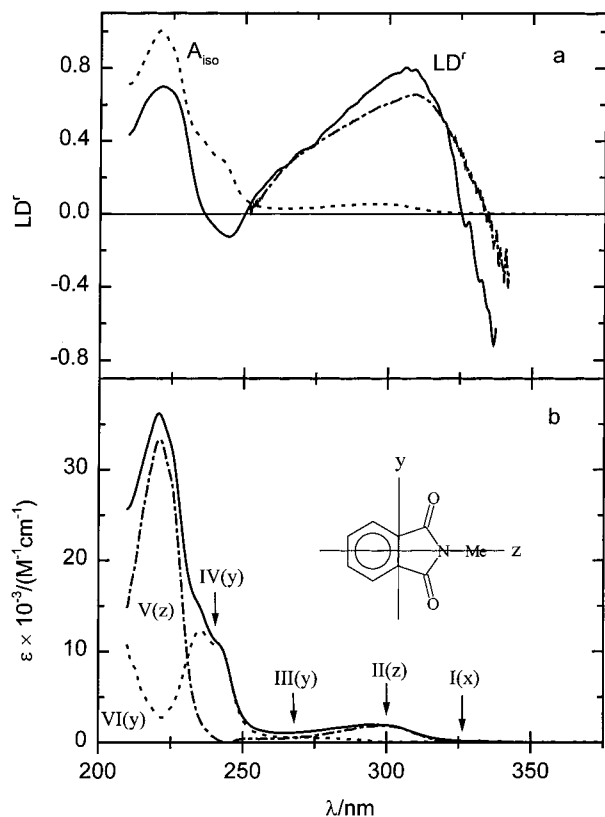


Figure 1. (a) UV isotropic absorption (A_{iso} , ---) and reduced linear dichroism (LD^f , —) spectra of **1b** in stretched PVA film at 20 °C. Also shown is the long-wavelength part of the LD^f spectrum (---) of **1c** in stretched PVA film measured on the same film as used in the IR LD experiment. (b) Resolved band shapes of the y - (---) and z -polarized (---) absorption intensities, and the isotropic absorption spectrum (—). The positions of the transitions I–VI are indicated with polarizations (x , y , or z) defined by the inserted molecular coordinate system.

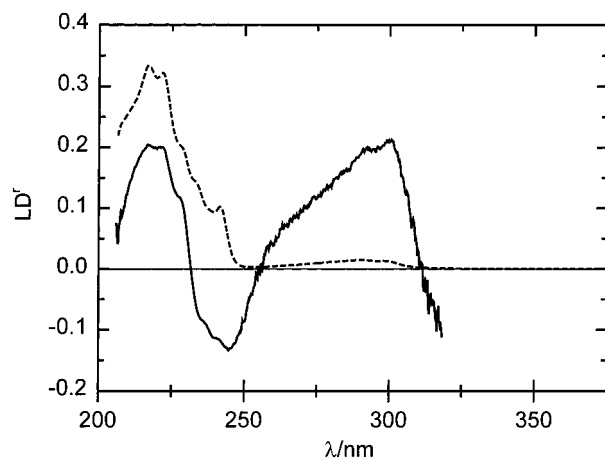


Figure 2. UV isotropic absorption (A_{iso} , ---) and reduced linear dichroism (LD^f , —) spectra of **1d** in stretched PE film at 20 °C.

of-phase carbonyl stretching vibrations, respectively.^{36,37} This assignment is confirmed in our calculations of vibrational spectra using density functional theory (DFT) at the B3LYP/6-31G-(d,p) level for compounds **1a** and **1b**. Since the phthalimide moiety can be regarded as having a local C_{2v} symmetry, these vibrations should be polarized along the C_2 -axis (in-phase combination, a_1 symmetry) or in the molecular plane perpen-

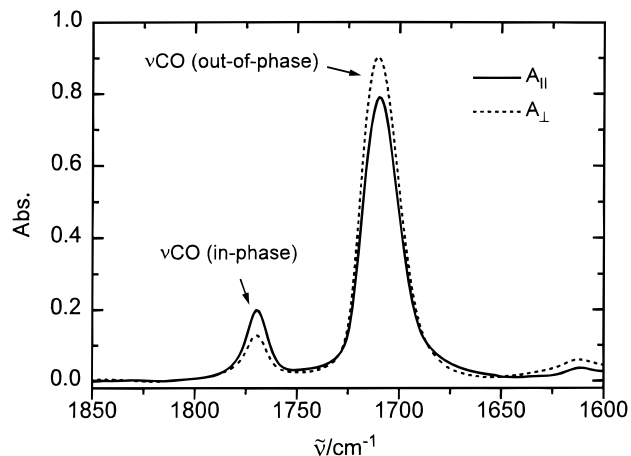


Figure 3. Polarized IR spectra, $A_{||}$ (—) and A_{\perp} (---), in the carbonyl stretching region of **1c** in stretched PVA film at 20 °C.

dicular to the long axis (out-of-phase combination, b_2 symmetry). If the molecules would orient with their long-axes (the z -axis in Figure 1b) as the principal orientation axis this would lead to an observed positive LD ($A_{||} > A_{\perp}$) for the in-phase vibration and a negative LD ($A_{||} < A_{\perp}$) for the out-of-phase combination. This is indeed what is observed so we conclude that all of the phthalimide derivatives included in the film studies orient with their long-axis aligned preferentially parallel with the stretching direction.

The in-plane orientation parameters are given directly from the observed extreme LD^f values at 245 and 305 nm for the in-plane transitions (vide infra) due to the symmetry of the molecules (eq 4). For **1a**, $S_{zz} = 0.19$ and $S_{yy} = 0.04$ giving $S_{xx} = -0.22$ according to eq 3. For **1b**, which is more elongated than **1a**, the S_{zz} is increased to 0.26, indicating a higher degree of orientation, and S_{yy} is correspondingly lowered to -0.04 . The $S_{xx} = -0.22$ which means that the out-of-plane orientation is about the same for **1a** and **1b**. For **1c**, the IR measurement gives $S_{zz} = 0.20$, $S_{yy} = -0.03$, and $S_{xx} = -0.17$. From the maximum LD^f value at about 305 nm we obtain $S_{zz} = 0.21$. In the case of **1d** in PE film, the overall orientation is lowered ($S_{zz} = 0.07$). Furthermore, the similarity of the LD^f values for the short-axis and out-of-plane polarized transitions at about 240 and 340 nm indicate that **1d** orients similar to a rod in stretched PE film.²⁴

The size of the order parameters is in very good agreement with what has been found in previous stretched film studies on molecules of similar size and shape.²³ Having considered the mode of orientation for the phthalimides, we now turn to a closer examination of the electronic absorption and polarized spectra.

The UV spectrum of the phthalimide chromophore is composed of two main regions: the low energy band (260–350 nm) with a low intensity ($\epsilon < 2000 \text{ M}^{-1} \text{ cm}^{-1}$) and the high energy band (200–260 nm) with rather intense transitions ($\epsilon_{max} = 36000 \text{ M}^{-1} \text{ cm}^{-1}$). At the red edge of the low energy band there is a very weak absorption tail going out to about 340 nm. The negative LD^f value at the red edge of the tail observed both for all of **1a–d** is direct evidence for an out-of-plane polarized transition probably due to an $n \rightarrow \pi^*$ transition (vide infra).

Assuming C_{2v} symmetry of the chromophore and using the orientation parameters obtained from the observed extreme LD^f values and the polarized absorption components ($A_{||}$ and A_{\perp}), the absorption spectrum of *N*-methylphthalimide (**1b**) was resolved into band shapes for the z - and y -polarized absorptions (Figure 1b). Starting at about 320 nm we have a weak long-

(36) Bree, A.; Edelson, M. *Spectrochim. Acta* **1981**, *37A*, 225.

(37) Arenas, J. F.; Marcos, J. I.; Ramirez, F. J. *Appl. Spectrosc.* **1989**, *43*, 118.

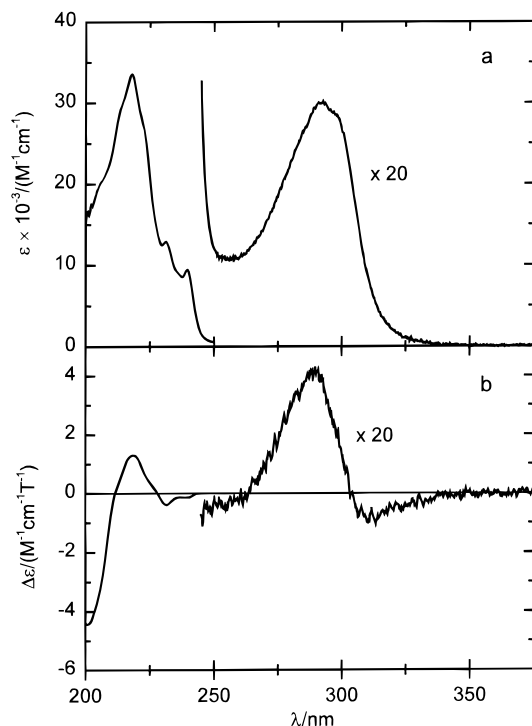


Figure 4. (a) UV absorption and (b) magnetic circular dichroism (MCD) spectrum of **1b** in ethanol at 20 °C. The sample concentrations were approximately 20 μM and 0.35 mM for the short and long wavelength parts of the spectra, respectively.

axis (z) polarized $\pi \rightarrow \pi^*$ transition giving rise to the observed maximum in LD^f at around 305 nm. This transition probably overlaps with a very weak $\pi \rightarrow \pi^*$ transition being short-axis (y) polarized and centered at about 275 nm. The overlap explains the gradual decrease in LD^f seen in the 260–300 nm region.

In the high energy region, we clearly observe three different $\pi \rightarrow \pi^*$ transitions. The first is seen as a shoulder in the absorption at about 245 nm but differs clearly in polarization from the main component of this strong band. The LD^f shows a distinct minimum over the shoulder at 245 nm, indicating that this transition is short-axis polarized. At 220 nm we observe a strong ($\epsilon \approx 33000 \text{ M}^{-1} \text{ cm}^{-1}$) long-axis polarized transition. The next transition at about 205 nm is of medium intensity and short-axis polarized. The positions of the transitions are indicated in Figure 1b.

In Figure 4, the A_{iso} and magnetic circular dichroism (MCD) of **1b** in ethanol is shown. The MCD is often used to obtain more information about the number transitions that contribute to a certain absorption band, and in the case of the phthalimide chromophore we expect to see a B-type spectrum where consecutive differently polarized transitions should give rise to a sign reversal in the MCD signal.³⁸ Over the weak low-energy absorption region, a bisignate MCD spectrum is observed where the first lobe extends over the weak absorption tail. The bisignate character of the MCD signal is a strong indication of at least one additional transition (at about 340 nm), responsible for the weak absorption tail, and that this transition is polarized perpendicular to the long-axis polarized $\pi \rightarrow \pi^*$ transition at 305 nm. There is no isolated feature in the MCD spectrum that could be ascribed to the very weak transition at about 270 nm, although there is a change in sign at 265 nm leading to a very weak negative MCD.

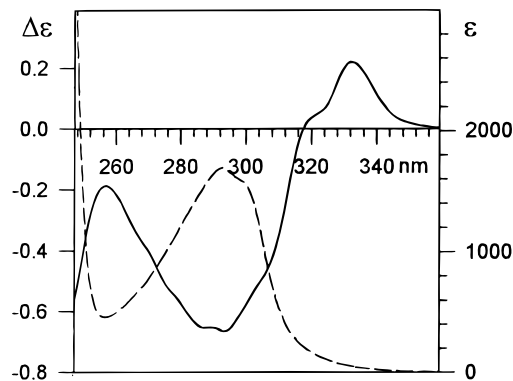


Figure 5. The long-wavelength portion of the CD (—) and UV absorption (---) spectra of **3b** in acetonitrile at 20 °C. The sample concentration was approximately 0.35 mM.

At higher energy, the MCD becomes negative over the 245 nm transition and is also showing vibrational structure as in the absorption spectrum. At 230 nm the MCD changes sign to be positive and has a maximum at 220 nm, and then there is another change of sign at 210 nm followed by a relatively strong minimum at 203 nm. Additional evidence for an isolated transition around 330 nm is found in the CD spectrum of the chiral phthalimide **3b** (Figure 5). It displays a weak positive Cotton effect at 331 nm whose position corresponds to the position of the presumed $n \rightarrow \pi^*$ band (vide infra). Furthermore, at higher energy the CD becomes negative and has a minimum at 295 nm probably corresponding to the long-axis polarized transition with a maximum at about 305 nm in the PVA film.

Comparison with Calculations. In Table 1, the observed electronic transitions are summarized and compared with the results from SCRF INDO/S-CI and CIS/6-31+G(d) calculations of the excited states. We find excellent agreement between experiment and the INDO/S calculation regarding the symmetry, energy, and polarization of the transitions. The only transition predicted in the studied wavelength interval that we do not observe experimentally is the $S_0 \rightarrow S_2$ transition (predicted at 318 nm) which is forbidden (A_2 symmetry). This transition corresponds to the excitation from a MO being mainly the out-of-phase combination of the lone pair orbitals of the carbonyl oxygens to a π^* orbital. Such a forbidden transition would not be observable as an isolated transition; however, it might acquire some intensity from vibronic borrowing from nearby allowed transitions and, thus, should have the same polarization as the latter. A similar pattern of low-lying $n \rightarrow \pi^*$ transitions as in the phthalimide chromophore has been observed by Xu and Clark for the related glutarimide chromophore.³¹

The effect of solvent polarity on the electronic transitions is found to be quite small since the absorption spectra of **1b** in PVA (Figure 1a) and of **1d** in PE (Figure 2) are very similar. This is seen also when comparing the gas-phase (not shown) and the SCRF INDO/S-CI results (Table 1). Only small red-shifts are found for the $\pi \rightarrow \pi^*$ transitions and small blue-shifts for the $n \rightarrow \pi^*$ transitions.

In the case of the CIS/6-31+G(d) calculation the agreement with experiment is fair. The main features of the absorption spectrum are reproduced, but the calculated ordering of some of the weak transitions seems to be wrong. This might be explained by that the CIS method treats electron correlation inadequately,⁴⁰ and, thus, excited states for which electron

(38) Nordén, B.; Håkansson, R.; Pedersen, P. B.; Thulstrup, E. W. *Chem. Phys.* **1978**, *33*, 355.

(39) Xu, S.; Clark, L. *J. Am. Chem. Soc.* **1994**, *116*, 9227.

(40) Foresman, J. B.; Head-Gordon, M.; Pople, J. A.; Frisch, M. J. *J. Phys. Chem.* **1992**, *96*, 135.

Table 1. Calculated and Observed Electronic Transitions of *N*-Methylphthalimide (**1b**)

trans.	SCRF INDO/S ^a				CIS/6-31+G(d) ^b				experimental			
	type	λ/nm	f^c	pol ^d	type	λ/nm	f^c	pol ^d	trans.	λ/nm	$\epsilon^e/\text{M}^{-1} \text{cm}^{-1}$	pol ^d
S ₀ →S ₁	n→ π^*	341	0.002	x	n→ π^*	298	0.0003	x	I	~350	~100	x
S ₀ →S ₂	n→ π^*	318	0.000	—	π → π^*	297	0.023	y				
S ₀ →S ₃	π → π^*	278	0.012	z	π → π^*	291	0.040	z	II	300	1840	z
S ₀ →S ₄	π → π^*	264	0.010	y	n→ π^*	275	0.0000	—	III	275	~500	y
S ₀ →S ₅	π → π^*	216	0.30	y	π → π^*	233	0.006	y	IV	237	12200	y
S ₀ →S ₆	π → π^*	211	0.96	z	π → π^*	225	0.92	z	V	221	33200	z
S ₀ →S ₇	π → π^*	196	0.59	y	π →s [*]	215	0.018	x	IV	~210	—	y

^a 120 singly excited configurations in CI. ^b Transition energies and oscillator strengths scaled with a uniform scale factor of 0.75. ^c Oscillator strength. ^d Polarization of transitions. See Figure 1b for the definition of molecular coordinate system. ^e Molar absorptivity in PVA film.

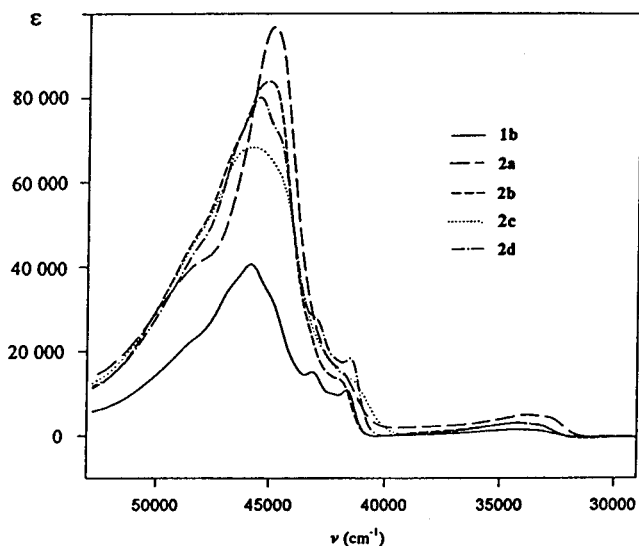


Figure 6. UV absorption spectra of *N*-methylphthalimide (**1b**) and of bis-phthalimides **2a–d** in acetonitrile at 20 °C. The sample concentration was approximately 10 μM .

correlation is important will be poorly described relative to states which can be described by configuration interaction with single excitations from the Hartree–Fock determinant. It should be noted that the *ab initio* calculated transition energies, and consequently the oscillator strengths, were scaled with a scale factor of 0.75 in order to facilitate comparison with experiment.

To summarize, we have presented a detailed picture of the number of electronic transitions in the UV region, their intensity distributions, and their polarizations. Of special interest from a theoretical point of view is the unambiguous assignment of an n π^* state as the lowest singlet excited state.

Exciton Coupling in the Electronic Spectra of Bis-Phthalimides 2a–d. Two phthalimide chromophores, linked through a short chain, should display electronic spectra differing from that of monomer **1b** due to the interchromophoric exciton coupling. The bis-phthalimides **2a–d** represent such systems, although not ideal. These molecules are nonrigid, and as a consequence any exciton coupling effect due to a particular conformer tends to be averaged over the contributions of other conformers. Fortunately, the number of conformers of significance with regard to the 220 nm π → π^* transition is reduced, as a result of collinearity of the electric transition moment with the direction of the N–C bond linking the phthalimide group to the rest of the molecule. While only one conformer sufficiently represents the low energy structures of **2a** and **2b**, trans and gauche conformers of **2c** and **2d** can contribute to the observed effects of exciton interactions in the electronic spectra. Figure 6 shows the UV absorption spectra of **2a–d** and that of **1b** for comparison.

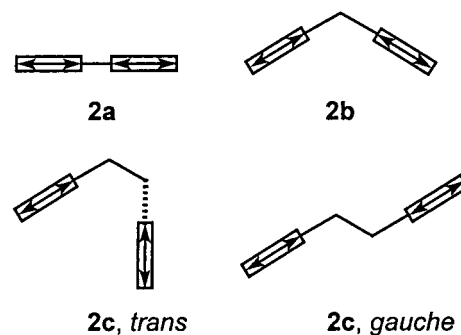


Figure 7. Schematic representation of the electric dipole transition moments of bis-phthalimides **2a–c**.

The UV spectrum of *N,N'*-bis-phthalimide (**2a**) differs significantly from that of **1b**. The absorption band near 45455 cm^{-1} (220 nm) is red-shifted by 1030 cm^{-1} . As the two phthalimide groups are directly connected, there is a question of conjugation between the two chromophores. The structure of this molecule in the solid state has been studied by Apreda *et al.* by X-ray diffraction analysis.⁴¹ It was found that the planes of the two phthalimide moieties are twisted with a dihedral angle of 78°. The N–N' bond length is 1.372 Å, which is shorter than typical single N–N bond (1.45 Å), but considerably longer than a typical N=N bond (1.25 Å). The large twist angle of the two planar halves of the dimer and the length of the N–N' bond indicate that the effect of conjugation between the two phthalimide chromophores can be neglected. Therefore, the red shift of the absorption maximum of **2a** is due to an in-line arrangement of the electric transition moments of the two phthalimide chromophores⁴² (Figure 7).

A small red shift (720 cm^{-1}) is seen also for dimer **2b**. For the methylene-linked dimer **2b** with the N–C–N bond angle equal to ca. 110°, the geometry of the two electric dipole transition moments is oblique, and band splitting results in an increased intensity of the lower energy component; this is observed as a net red shift of the absorption maximum. The trans-conformer of **2c** would have effectively no effect on the absorption maximum of the dimer because of the separation of the two electric dipoles. On the other hand, the gauche conformer of **2c** contributes to the electronic spectrum mainly through band-splitting. The latter effect is experimentally observed as a lowered extinction coefficient; ϵ_{max} of dimer **2c** is 16% lower than twice the ϵ_{max} value of monomer **1b**. In the case of the trimethylene analogue **2d**, no exciton coupling is evident from the absorption spectrum; it resembles closely the sum of the absorption spectra of the two **1b** monomers.

(41) Apreda, M. C.; Foces-Foces, C.; Cano, F. H.; Garcia-Blanco, S. *Acta Crystallogr.* **1978**, *B34*, 3477.

(42) Kasha, M.; Rawls, H. R.; El-Bayoumi, M. A. *Pure Appl. Chem.* **1966**, *11*, 371.

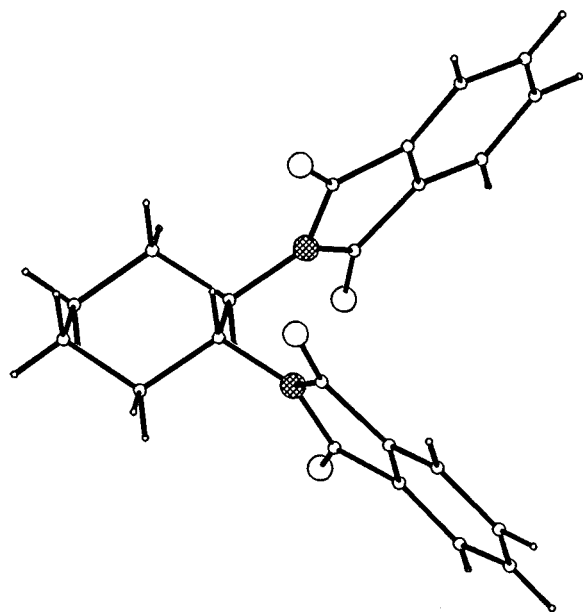


Figure 8. Perspective view of one of two crystallographically independent molecules of **3a**. The biggest open circles represent O atoms, the shaded N atoms. The two molecules, each possessing a 2-fold rotation axis coinciding with the crystallographic dyad, are very similar.

In summary, the small but distinct differences in the position of the absorption maximum of bis-phthalimides **2a–c** could be qualitatively accounted in terms of exciton coupling of the electric dipole transition moments of the 220 nm transition, polarized along the long axis of the phthalimide molecule.⁴³

Degenerate Exciton Coupling in the CD Spectra of Phthalimides. We studied both the "rigid" model compound **3a** and the conformationally flexible molecule **4a**. The degenerate exciton coupling case represented by bis-phthalimide **3a** is of special interest as it demonstrates the appearance of exciton-split Cotton effects in the region of the allowed $\pi\text{--}\pi^*$ transitions below 260 nm. These Cotton effects are of great importance for unambiguous determination of stereo-structure of the bichromophoric system and, hence, for determination of absolute configuration and conformation of the molecule. An advantage of the phthalimide chromophore is that the direction of the electric dipole transition moment for the strongly allowed 220 nm transition is basically collinear with the direction of the C–N connecting bond and is invariant to any rotation of the C–N bond.

Details of the structure of bis-phthalimide **3a** of known (1*R*,2*R*) absolute configuration have been obtained by X-ray diffraction analysis (Figure 8). In the crystal structure the cyclohexane rings adopt nearly ideal chair conformations with phthalimide rings in diequatorial orientation. The torsional angles describing mutual orientation of the phthalimide rings are as follows: $\angle N(1)\text{--}C(9)\text{--}C(9a)\text{--}N(1a) = -54.9(3)^\circ$, $\angle N(1')\text{--}C(9')\text{--}C(9a')\text{--}N(1a') = -53.9(3)^\circ$ for the two independent molecules. Letter "a" denotes atoms related by a 2-fold symmetry axis. The C–H bonds at the chiral centers are nearly parallel to one of the two C=O bonds; the angles between the lines defined by these bonds amount to 15.9 and 9.8°, in unprimed and primed molecule, respectively. The phthalimide moieties, although roughly planar, differ slightly in the degree of planarity in both molecules; the root-mean-square deviation

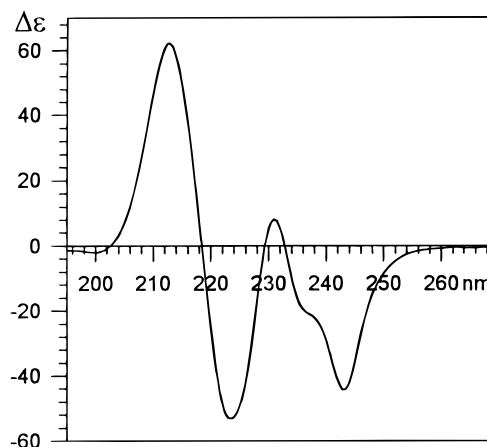


Figure 9. CD spectrum of **3a** in acetonitrile at 20 °C. The sample concentration was approximately 10 μM .

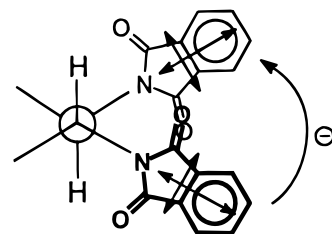


Figure 10. Degenerate exciton coupling of the two $\pi\text{--}\pi^*$ transitions polarized along short and long axes of the phthalimide chromophore in **3a**.

of the fitted atoms amounts to 0.022 and 0.003 Å, in the unprimed and primed molecule, respectively.

The CD spectrum of **3a** (Figure 9) displays two sets of exciton-type Cotton effects around 218 and 240 nm which correspond to the position of absorption maximum at 216 nm and a shoulder at 240 nm in the UV spectrum. The two sets of Cotton effects are, accordingly, due to the long-axis polarized (216 nm) and short-axis polarized (240 nm) transitions, and their negative signs are qualitatively accounted for⁴⁴ in Figure 10. Both degenerate couplings lead to negative Cotton effects reflecting the negative gauche torsional angle of the N–C–C–N bond system. The 240 nm CD bands are unsymmetrical due to the cancelation effect of the closely lying CD bands and possibly due to the presence of another CD band in this region.

From the approximate band shapes obtained from the analysis of the short-axis and long-axis polarized absorption components of **1b** (Figure 1b), we estimate the size of the transition dipoles for the 216 and 240 nm transitions to be 5.09 and 0.32 D, respectively. These values together with the geometrical information from the crystal structure were used in a coupled-oscillator calculation⁴⁴ of the rotatory strength and exciton splitting for **3a**. The calculated rotatory strengths are up to 70% larger than those estimated from the CD spectrum of **3a**. Taking into account cancelation effects due to overlapping intensities of opposite sign, the agreement between the experiment and the calculation must be considered as satisfactory.

The conformationally flexible bis-phthalimide **4a**, a derivative of 1,2-diaminopropane of (*R*)-configuration, has a CD spectrum very similar both in shape and in magnitude to that of **3a** (Table 2). **4a** is expected to occur in either the (–)-gauche, (+)-gauche, or trans conformations of the N–C–C–N bond system or

(43) Through-space and through-bond effects on exciton interactions between rigidly linked naphthalene molecules have been recently demonstrated: Scholes, G. D.; Ghiggino, K. P.; Oliver, A. M. Paddon-Row, M. N. *J. Am. Chem. Soc.* **1993**, *115*, 4345.

(44) (a) Rodger, A.; Nordén, B. *Circular Dichroism and Linear Dichroism*; Oxford University Press: Oxford, 1997; Chapters 5 and 7.7. (b) Harada, N.; Nakanishi, K. *Circular Dichroic Spectroscopy – Exciton Coupling in Organic Stereochemistry*; University Science Books: Mill Valley, CA, 1983.

Table 2. CD Maxima of Compounds **4a–c** and **5b**

compound	Cotton effects, $\Delta\epsilon$ (nm)		
4a	-34.5 (242)	-70.0 (225)	+60.5 (213)
4b^{a,b}	+7.4 (240)	-26.2 (225)	+7.4 (214)
4c^a	+2.0 (242)	-26.2 (227)	+10.7 (216)
5b	+2.0 (242)	-27.4 (227)	+11.6 (215)

^a From ref 15. ^b The enantiomer of this compound was prepared.

possibly as a mixture of all three conformers. Of these, only the (-)-gauche and (+)-gauche conformers would give any exciton CD. The similarity between the CD spectra of **4a** and **3a** indicates that **4a** prefers the (-)-gauche conformation (Figure 10). The (+)-gauche conformer should be destabilized by crowding of the substituents, and it would be incompatible with the observed ¹H NMR coupling constants (see Supporting Information).

Additional support for this conclusion comes from theoretical calculations of the stability of the various conformers of **4a**. After an initial search with the MM+ and AM1 methods for the lowest energy conformers having (-)-gauche, (+)-gauche, and trans configuration of the N–C–N bond system, the lowest energy structure for each configuration was selected for full geometry optimization using HF/6-31+G(d) theory. All three methods predict the (-)-gauche configuration to be clearly the most stable with the N–C–N torsional angle calculated at the HF/6-31+G(d) level to -67.7°. The HF/6-31+G(d) energy difference relative the (-)-gauche conformer is +7.1 kJ/mol and +8.7 kJ/mol for the (+)-gauche and trans forms, respectively. The corresponding MM+ and AM1 energy differences are, respectively, MM+: +9.2 kJ/mol and +13.7 kJ/mol and AM1: +5.2 kJ/mol and +5.2 kJ/mol. The similarity between the results of the molecular mechanics and the ab initio calculations indicates that steric hindrance is the main reason for the higher energy of the (+)-gauche conformer.

Nondegenerate Exciton Coupling in the CD Spectra of Phthalimides. Nondegenerate coupling of the excited states of the phthalimide chromophore with the excited states of other chromophores of comparable excitation energy has great potential for determining the absolute stereo-structure of amino alcohols (phthalimide–benzoate coupling) and aromatic amines (phthalimide–phenyl coupling).^{15,16} We have investigated two “rigid” model compounds, **3c** and **3d**, representing two cases of nondegenerate exciton coupling. Both compounds are structural analogues of the bis-phthalimide **3a**, having one phthalimide group replaced by a benzoate (**3c**) or a phenyl group (**3d**), with preserved absolute configuration. As seen in Figure 11 both compounds display negative exciton-split Cotton effects centered around absorption maxima of each participating transition. Namely, in the case of phthalimido-benzoate **3c**, the negative Cotton effect at 228 nm corresponds to the $\pi \rightarrow \pi^*$ transition of the benzoate, polarized parallel with the direction of the C–O bond, while the positive Cotton effect at 215 nm is due to the long-axis polarized $\pi \rightarrow \pi^*$ transition of the phthalimide chromophore. The weak CD band at 241 nm is due to the coupling of the short-axis polarized phthalimide transition and benzoate $\pi \rightarrow \pi^*$ transition, and it represents the lower energy part of the positive exciton-split Cotton effect. This Cotton effect is of opposite sign to the exciton Cotton effect around 220 nm due to the orthogonality of the participating long- and short-axis polarized transitions in the phthalimide chromophore.

In the case of phthalimide **3d**, the negative Cotton effect at 220 nm is due to the long-axis polarized phthalimide transition while the positive Cotton effect at ca. 206 nm is due to the ¹L_a

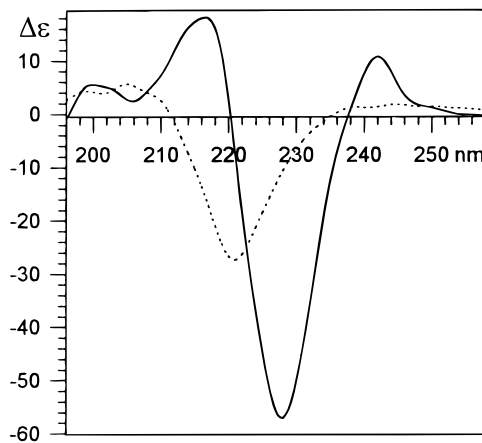


Figure 11. CD spectra of phthalimides **3c** (—) and **3d** (····) in acetonitrile at 20 °C. The sample concentration was approximately 10 μ M.

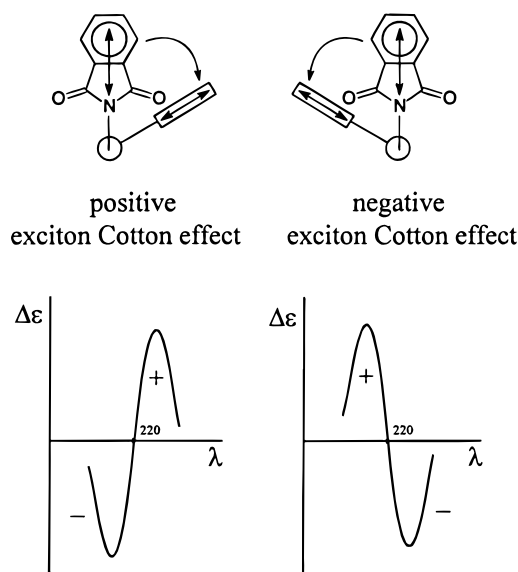


Figure 12. Relationship between the sign of exciton Cotton effects and the absolute configuration.

transition in the phenyl chromophore which is also long-axis polarized, i.e., it is collinear with the C–C bond connecting the phenyl and the cyclohexane rings. In this case a very weak Cotton effect could be observed in the 240 nm region. This is because the coupling of the short-axis polarized phthalimide and ¹L_a phenyl transitions is weak, as the result of a larger energy gap separating the two transitions. Thus, in both cases, **3c** and **3d**, the CD spectra unequivocally reflect the chirality of the bichromophoric system.

Equally conclusive are the results of analysis of the CD spectra of conformationally flexible phthalimido-benzoate aminopropanol derivatives **4b** and **4c** of the same (*R*)-configuration. Regardless of the site of attachment of the phthalimido group, whether to the primary or to the secondary carbon atom, the resulting exciton-split Cotton effects (Table 2) are negative, in accordance with the absolute (*R*)-configuration and the preferred (-)-gauche conformation of the O–C–N bond system (see the discussion of the degenerate case **4a**). In Figure 12, we summarize the above findings regarding the correlation between the signs of the exciton Cotton effects and the absolute configuration of the molecules.

Finally, an example of the practical application of the interpretation of exciton-coupled phthalimide Cotton effect for

determination of absolute configuration. Compound **5a** was obtained by Šunjić⁴⁵ by enzymatic kinetic resolution of the racemic acetate, as a three-carbon building block for the synthesis of β -androgenic blockers. However, the absolute configuration was not determined. By converting the hydroxyl group in **5a** to the benzoyl ester in **5b**, it was possible for us to utilize phthalimide–benzoate nondegenerate exciton coupling to indirectly determine the absolute configuration of **5a**. As shown in Table 2, **5b** displays negative exciton-split Cotton effect due to nondegenerate coupling of the long-axis polarized phthalimide $\pi \rightarrow \pi^*$ and benzoate $\pi \rightarrow \pi^*$ transitions, with amplitude similar to that of **4c**. This unequivocally establishes negative helicity of the N–C–C–O bond system and (S)-configuration of **5a**.

Conclusions

The UV spectrum of the phthalimide chromophore has been investigated using polarized light spectroscopy and quantum chemical calculations. A weak $n \rightarrow \pi^*$ transition (I) polarized out of the molecular plane is found as the lowest lying transition at about 340 nm. At higher energy we assign five in-plane polarized $\pi \rightarrow \pi^*$ transitions: II (300 nm, z-pol), III (275 nm, y-pol), IV (235 nm, y-pol), V (220 nm, z-pol), and VI (~210 nm, y-pol). These results should be useful for practical applications, such as structural applications of CD and LD

spectroscopy, but also of help for validating and developing theoretical methods for an accurate description of heterocyclic molecules.

On the basis of spectroscopic and theoretical assignments, we have formulated and confirmed experimentally a nonempirical method for determining the absolute stereo-structure of diamines, amino alcohols, and aromatic amines. The method requires converting the amine to the *N*-phthaloyl derivative (and the alcohol into the *O*-benzoyl derivative) and recording the Cotton effects due to the exciton-coupled long-axis polarized phthalimide transition IV at ca. 220 nm. The chirality of the system is simply and unequivocally determined from the sign of the exciton-split Cotton effect.

Acknowledgment. We thank Dr. J. Frelek for providing the CD spectra. We are grateful to Dr. H. Takada for a sample of (1*R*,2*R*)-2-aminocyclohexanol and to Dr. V. Šunjić for a sample of **5a**. Financial support from the Polish Committee for Scientific Research (KBN), Grant No. PB 265/T09/95/08, and the Swedish Natural Science Research Council is gratefully acknowledged. A.H. would like to thank the Chemistry Section at Chalmers University for a Postdoctoral Research Fellowship.

Supporting Information Available: A listing of synthetic procedures (5 pages, print/PDF). See any current masthead page for ordering information and Web access instructions.

(45) Šunjić, V.; Gelo, M. *Synthesis* **1993**, 855.